

USING MOLTEN-SALT ENERGY STORAGE TO DECREASE THE MINIMUM OPERATION LOAD OF THE COAL-FIRED POWER PLANT

by

**Yiwei FU^{a*}, Zhe NING^a, Weichun GE^b, Qingwei FAN^a,
Guiping ZHOU^b, and Tingshan MA^a**

^aXi'an Thermal Power Research Institute Co., Ltd., Xi'an, China;

^bState Grid Liaoning Electric Power Supply Company Limited, Shenyang, China

Original scientific paper

<https://doi.org/10.2298/TSCI191015009F>

As the renewable energy fluctuating in the power grid, the traditional coal-fired power plant needs to operate on the extremely low load, so as to increase the share of renewable energy. This paper deals with thermodynamic simulation and exergy analysis of the coal-fired power plant integrated with the molten-salt energy storage system to explore the potential of reducing the minimum operation load. A steady-state simulation was performed to obtain the thermodynamic properties of process streams in a subcritical 600 MW unit. The results indicated that with simple main steam and re-heat steam energy storage plan, the storage efficiencies are 39.4-42.9% and 51.3-51.4%, the minimum operation load would decrease by 27.2 MW, 10.6 MW, respectively. Exergy analysis shows that the exergy loss mainly comes from the throttling process and temperature difference in the phase-changer heat transfer process. With optimized Molten-salt energy storage plans, the storage efficiencies increase to 72.6% and 78% via lead the exhaust drains or steam into higher pressure points; the minimum operation load decreases by 35.1 MW and 3 MW, respectively. Moreover, with the coupled plan including both optimized main steam and re-heat steam energy storage system, the minimum operation load would decrease by 80.7 MW, and storage efficiency is 75.1%.

Keywords: molten salt thermal storage, coal-fired power plant, flexibility, simulation, thermodynamics analysis

Introduction

As renewable energy rapidly developing in the electricity market, it is an arising issue to solve the balance problem in the power grid caused by the fluctuation of renewable energy. To keep the balance between energy production and demands, the traditional coal-fired power plant (CFPP) is required to be more flexible [1]. Expanding the operation range of CFPP is the key factor in how much renewable energy could be consumed. For example, when the renewable energy production is relatively high in a certain power grid, it requires to decrease the power output of CFPP, so the average carbon emission of the power grid would be lower. But from the perspective of safe operation in CFPP, it has to operate

*Corresponding author, e-mail: yiwei fuyiwei691@outlook.com

above the minimum operation load (MOL) to keep the combustion in the boiler steady and safe.

To solve the contradiction between power demands and production, different energy storage forms have been proposed, including pumped hydro plants, compressed air energy storage, battery systems, and other technology that is still in development [2-4].

Molten-salt energy storage (MSES) has become a hot topic in recent years [5]. It is widely used in concentrating solar power plants, where it provides dispatchability [6, 7]. Considering that the CFPP is still urgent to achieve more flexibility to meet the rapid development of renewable energy, to integrate thermal energy storage (TES) system into CFPP is a promising way to reduce the minimum load and avoid overnight shutdowns, so as that the renewable energy consumption ability could be increased [8].

However, the researches presented in literature do not include how to use TES integrated with CFPP to reduce the MOL and its storage efficiency. Considering that the complexity of flue gas cycle equipment and low exergy efficiency of using electricity to heat molten salt, it is better to integrate the MSES system with the steam cycle. Therefore, the focus of this context lies on thermodynamic process analysis and optimization of the TES to explore the storage efficiency of TES integrating in the CFPP. To achieve this goal, the energy and exergy analysis model of the CFPP and TES was developed to calculate the energy and exergy loss distributions and component exergy efficiencies. Based on the simulation results, the storage efficiencies of different MSES plans were compared. Then the exergy loss distribution in the subsystems of the MSES and the CFPP was calculated. Furthermore, optimization proposals were put forward after the determination of the exergy loss sources in the MSES. Finally, a comprehensive performance assessment was conducted to investigate the influence of MSES on system performances, including MOL reduction and energy storage efficiency.

Integration of MSES with CFPP

As shown in figs. 1 and 2, in the reloading cycle, the cold salt (r_3) is heated by the steam ($r_1 \Rightarrow r_2$) and stored in the hot tank (r_4). In the unloading process, the hot salt (u_3) heats the feed water or cold re-heat steam ($u_1 \Rightarrow u_2$), and then goes back into the cold tank (u_4).

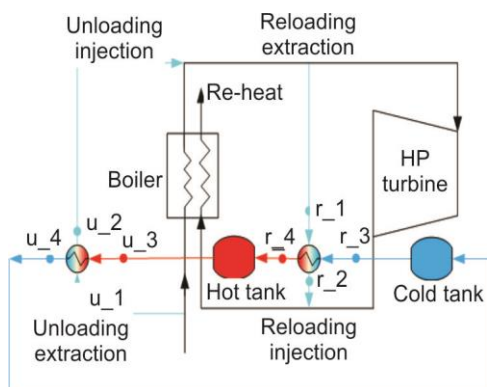


Figure 1. Main steam energy storage plan

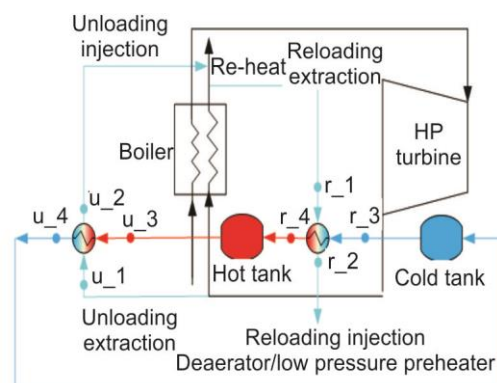


Figure 2. Re-heat steam energy storage plan

Simulation method

Reference case

In our study, a 600 MW subcritical CFPP was selected. The total power system has two main subsystems: the boiler and turbine. The main steam parameter is 16.67 MPa/538 °C with a rated load (THA) mass-flow 1760.2 t/h. The re-heat steam parameter is 3.28 MPa/538 °C, with a rated load mass-flow 1504.2 t/h. In 30% of the rated load and below, the re-heat temperature decreases to 510 °C, and the main steam temperature keeps the same as in the rated load.

To keep the combustion in the boiler steady, the design MOL is 30% of the rated load (30% THA), so when power output command is lower than 30% THA, the storage system's reloading process should be put into operation, then the boiler would keep at 30% of its rated load, but the turbine and electric generator would be running at a lower load. In order to release the stored energy, when the power output command is higher than 75% of the rated load, the boiler would keep at 75% of its rated load, then the turbine and the electric generator would be running at a higher load.

The CFPP model based on EBSILON

To analyze the performance of different energy storage plans and storage efficiency, a precise off-design thermal balance calculation should be carried out. In this section, the main models used in the thermodynamic analysis are developed. EBSILON [9], a universal heat balance calculation software, was used in this study. Figure 3 shows the simplified description of EBSILON units.

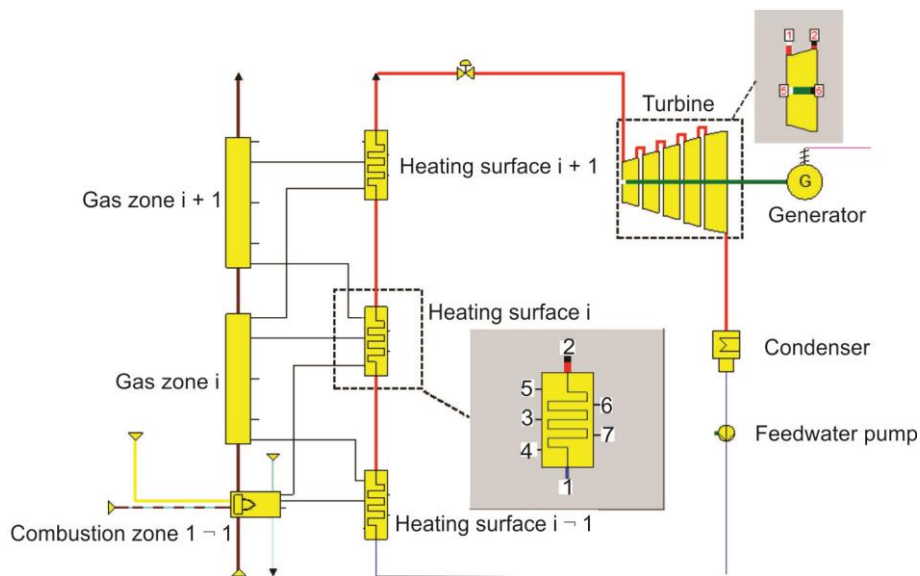


Figure 3. Simplified description of the power plant model built with EBSILON

Boiler heat balance model

As shown in fig. 3, the boiler consists of a series of heating surfaces. For heating surface I, the general energy governing equations are described:

$$m_1 = m_2 \quad (1)$$

$$(kA)LMTD + QR_{i-1} + QR_{i+1} = m_2 h_2 - m_1 h_1$$

where m_1 and m_2 [kg s^{-1}] are the mass-flow of the heating surface inlet and outlet, respectively, h_1 and h_2 [kJ kg^{-1}] are the mass-flow of the heating surface inlet and outlet, respectively, A [m^2] – the area of the heating surface, k [$\text{W m}^{-2} \text{°C}^{-1}$] – the heat transfer coefficient, which can be calculated based on geometric data of the heating surface, $LMTD$ [°C] – the mean logarithmic temperature difference, and QR_{i-1} and QR_{i+1} [W] are the radiation flow from predecessor and successor gas zone, respectively.

Turbine unit model

For the thermodynamic calculation of the steam turbine, the following assumptions were adopted:

- The efficiencies of the steam turbines are the same.
- The terminal temperature difference for the heaters of the regenerative system remains unchanged.

The model calculates the shaft work conducted on or by the blades of the stages based on the thermodynamic properties at each stage inlet and exhaust. The governing equations are described:

$$const = m_1 \sqrt{\frac{p_1}{v_1}} \quad (2)$$

$$W = m_1 (h_1 - h_2)$$

where m_1 [kg s^{-1}] is the inlet mass-flow, p_1 [MPa] – the inlet pressure, v_1 [$\text{m}^3 \text{s}^{-1}$] – the inlet volume flow, and h_1 and h_2 [kJ kg^{-1}] are the inlet and outlet enthalpy.

Model validation

The boiler-turbine coupled models were developed and depicted in fig. 4. In this study, the simulation results and design data were compared based on the main parameters of the power unit in the steady-state at four different working conditions. The results are illustrated in tab. 1. It turns out that the simulation results of the main parameters are consistent with the design data, and the maximum relative error is 1.17%, thereby validating the precision of our models in the steady-state.

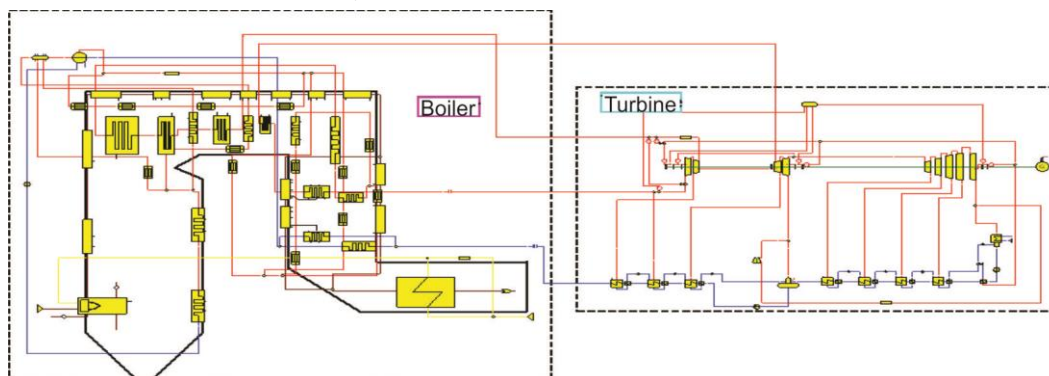


Figure 4. Boiler-turbine integration calculation model based on EBSILON

Table 1. Comparison of simulated result with design data at different working conditions

Parameters	THA			75% THA			50% THA			30% THA		
	Design data	Simulation	Relative error [%]	Design data	Simulation	Relative error [%]	Design data	Simulation	Relative error [%]	Design data	Simulation	Relative error [%]
Power [MW]	600.0	598.6	0.23	445.7	442.7	0.66	292.0	289.5	0.88	177.2	177.0	0.09
Main steam pressure [MPa]	16.67	16.60	0.42	13.89	13.94	-0.37	9.26	9.34	-0.89	7.41	7.44	-0.46
Main steam mass-flow [th ⁻¹]	1760.2	1754.5	0.33	1277.4	1266.4	0.86	834.1	832.6	0.18	530.3	525.8	0.85
Re-heat steam pressure [MPa]	3.28	3.25	0.99	2.44	2.44	-0.05	1.63	1.62	0.60	1.03	1.04	-1.17
Re-heat steam mass-flow [th ⁻¹]	1504.2	1502.7	0.10	1111.3	1114.2	-0.26	739.3	731.4	1.09	475.6	479.7	-0.85
Turbine exhaust enthalpy [kJkWh ⁻¹]	2306.4	2303.4	0.13	2340.4	2331.6	0.38	2412.2	2433.2	-0.87	2495.9	2486.1	0.40
Boiler exhaust gas temperature [°C]	125.0	125.6	-0.49	117.8	117.2	0.43	112.0	112.3	-0.30	93.0	92.0	1.02

The MSES subsystem model

Thermodynamic model

The MSES models are used to calculate the thermodynamic parameters and performance via the different plans of the MSES. The following assumptions are used as design principles:

- The minimum heat transfer temperature difference is set at 5 °C.
- In the reloading process, the injection steam temperature (u_2) is the same as the mixing point; in the unloading process, the injection steam temperature (r_2) is 15 °C lower than the mixing point.
- The molten-salt mass-flow is the same in the reloading and unloading cycles, which means the reloading and unloading speed of the storage system is the same.
- Take the storage heat loss into consideration; the storage temperature is 3 °C lower than the outlet salt temperature of the reloading heat exchanger:

$$\begin{cases} T_{u_1} = T_{u_extraction} \\ T_{u_2} = T_{u_injection} - 15 \\ T_{u_3} = T_{u_2} + 5 \\ T_{u_3} = T_{hot_salt} = T_{r_4} - 3 \\ m_{u_salt} (T_{u_3} - T_{u_4}) = m_{u_steam} (T_{u_2} - T_{u_1}) \end{cases} \quad \begin{cases} T_{r_1} = T_{r_extraction} \\ T_{r_2} = T_{r_injection} \\ T_{r_3} = T_{r_2} - 5 \\ T_{r_3} = T_{cold_salt} = T_{u_4} - 3 \\ m_{r_salt} (T_{r_4} - T_{r_3}) = m_{r_steam} (T_{r_1} - T_{r_2}) \end{cases} \quad (3)$$

where T_{u_i} and T_{r_i} [°C] ($i = 1, 2, 3, 4$) are the temperatures in the MSES system in fig. 1, m_{u_salt} and m_{u_steam} [kgs⁻¹] are the molten-salt and steam mass-flow in the unloading process, m_{r_salt} and m_{r_steam} [kgs⁻¹] are the molten-salt and steam mass-flow in the reloading process, $T_{u_extraction}$ and $T_{u_injection}$ [kgs⁻¹] are the steam extraction point, and the injection point in the unloading process, and T_{hot_salt} and T_{cold_salt} [°C] are the molten-salt storage temperature in the tanks.

Exergy analysis

The substances of the MSES system include steam and molten-salt. In the exergy analyses, the reference pressure and temperature are taken respectively as 0.1 MPa and 423.15 K.

The exergy of steam or water is calculated with:

$$e = h - h_0 - T_0 (s - s_0) \quad (4)$$

where h [kJkg^{-1}] is the enthalpy of the working substance, h_0 [kJkg^{-1}] – the enthalpy of the working substance under reference condition, s [$\text{kJkg}^{-1}\text{°C}^{-1}$] – the entropy of the working substance, and s_0 [$\text{kJkg}^{-1}\text{°C}^{-1}$] – the entropy of the working substance under reference condition.

Result and discussion

The following results are assuming that take 75% THA as the unloading base load, 30% THA as the reloading base load, and keep the energy into the boiler unchanged.

Operational limitation

The energy storage plan should not affect the safe and stable operation of CFPP. The key factors which should be considered include avoiding boiler overheating issue and ensuring turbine axial thrust within the safety range, and these factors determine the reduction of the MOL.

Reloading limitation

In the reloading cycle, extraction steam from the main steam or the re-heat steam would change the axial thrust balance of the turbine unit, and getting worse as the extraction mass-flow increases, to ensure the axial thrust within the safe range, there should be an upper limit in the reloading process.

For the main steam storage shown in fig. 1, based on the design data provided by the turbine manufacturer, the maximum steam extraction capacity is 10% of the main steam mass-flow of rated load condition, which is approximately 176 t/h based on the design parameters. As shown in tab. 2, the minimum load decrease is 27.2 MW, which is about 4.5% of the rated load.

As to the re-heat steam storage plan in fig. 2, based on the thermal balance calculation for the power plant in the 30% of rated load, the total extraction steam of deaerator and low pressure preheaters is 76.4 t/h, which is much lower than the mass-flow that would cause axial thrust balance issue. Therefore, the limit depends on the steam consumption of deaerator and low pressure pre-heaters. The simulation results of the storage system are shown in tab. 2. The result shows that 10.6 MW reduction of minimum load, which is about 1.8% of the rated load.

Unloading limitation

In the unloading cycle, because the MSES system provides steam instead of the boiler, the main steam and re-heat steam would not change simultaneously, then the re-heat steam or main steam temperature might increase or decrease.

As shown in figs. 5 and 6, the main steam mass-flow nearly remains unchanged, but the re-heat steam mass-flow increases with the increase of steam generation from MSES in the main steam energy storage plan. It would cause the re-heat temperature to decrease, and

Table 2. Reloading limitations of different storage plans

Thermal parameter	Main steam energy storage	Re-heat steam energy storage
Electric power decrease [MW]	27.2	10.6
Hot salt storage temperature [°C]	530.0	502.0
Cold salt storage temperature [°C]	292.0	320.0
Molten-salt mass-flow [th ⁻¹]	240.0	100.0
Extraction steam mass-flow [th ⁻¹]	176.0	76.4
$T_{r,1}$ [°C]	538.0	510.0
$T_{r,2}$ [°C]	343.8	331.9
$T_{r,3}$ [°C]	292.0	320.0
$T_{r,4}$ [°C]	533.0	505.0

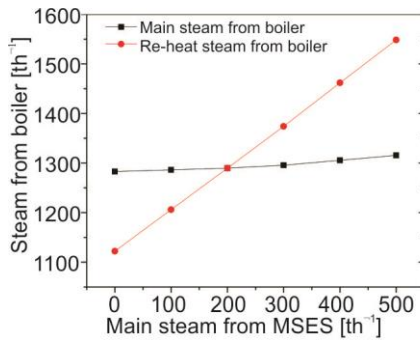


Figure 5. Steam generation from boiler with main steam energy storage

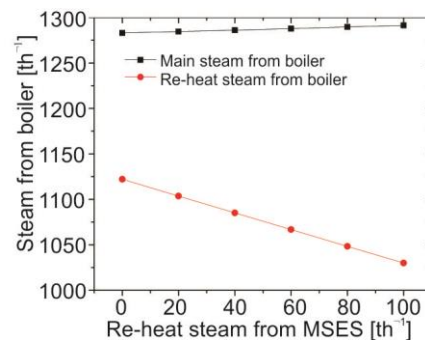


Figure 6. Steam generation from boiler with re-heat steam energy storage

the turbine exhaust humidity increase. Therefore, the unloading limitation is to ensure the exhaust humidity smaller than the maximum value at normal working conditions, which is 0.1 based on the design data. The simulation results in fig. 7 and tab. 3 show that the maximum generation steam from MSES in 415 t/h, the re-heat temperature is 502.9 °C, the electricity power increases from 445.7 MW to 560.7 MW. The maximum load increase is 115.0 MW, which is about 19.2% of the rated load.

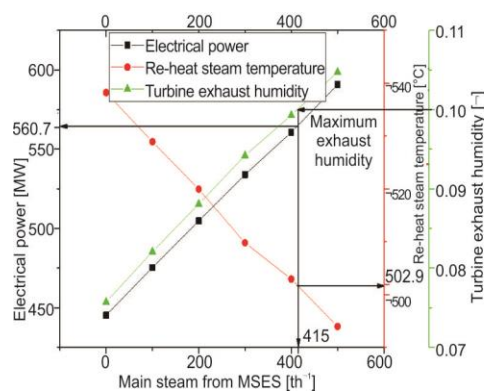


Figure 7. Operational limit in the unloading process for the main steam energy storage system

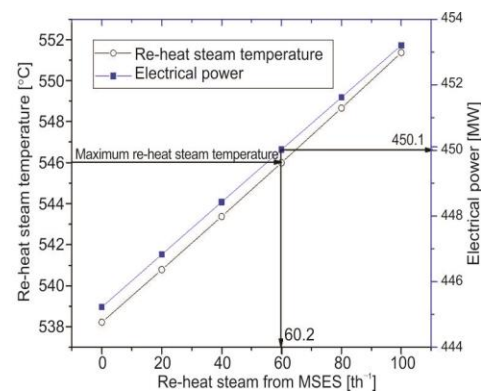


Figure 8. Operational limit in the unloading process for the reheat steam energy storage system

On the contrary, in the re-heat steam energy storage plan, the re-heat steam mass-flow would decrease and cause re-heat temperature higher than the design value. The boiler temperature is designed 3 °C higher than the turbine inlet temperature (538 °C) and considering the safety requirement, the steam temperature could vary within 541 ±5 °C, the maximum steam temperature should be 546 °C. The simulation results in fig. 8 and tab. 3 show that the maximum generation steam from MSES is 60.2 t/h, the electricity power increases from 445.7 MW to 450.1 MW. The maximum load increase is 4.4 MW, which is about 0.73% of the rated load.

Table 3 Unloading limitations of different storage plans

Thermal parameter	Main steam energy storage	Re-heat steam energy storage
Electric power increase [MW]	115.0	4.4
Hot salt storage temperature [°C]	530.0	502.0
Cold salt storage temperature [°C]	292.0	320.0
Molten-salt mass-flow [th ⁻¹]	2587.0	87.8
Extraction steam mass-flow [th ⁻¹]	415	60.2
$T_{u,1}$ [°C]	256.1	317.3
$T_{u,2}$ [°C]	525.0	497.0
$T_{u,3}$ [°C]	530.0	502.0
$T_{u,4}$ [°C]	295.0	323.0

Storage efficiency and exergy analysis

Assuming the MSES system working in a steady-state, the storage efficiency definition:

$$\eta_s = \frac{W_u - W_{ub} \frac{t_u}{t_r}}{W_{rb} - W_r \frac{t_u}{t_r}} = \frac{W_u - W_{ub} \frac{M_r}{M_u}}{W_{rb} - W_r \frac{M_r}{M_u}} \quad (5)$$

where W_{rb} [MW] is the original output power of baseload in the reloading process, W_r [MW] – the output power in the reloading process, W_u [MW] – the output power in the unloading process, W_{ub} [MW] – the original output power of baseload in the unloading process, t_u and t_r [s] are the unloading and reloading working time in a complete cycle of the storage period, respectively, and M_u and M_r [kgs⁻¹] are the molten-salt mass-flow in the unloading and reloading processes, respectively.

Storage efficiency

The storage efficiencies under different reloading and unloading speeds are listed in tabs. 4 and 5. The simulation results show that the efficiency is higher with lower unloading speed and higher reloading speed. For the main steam energy storage plan, the efficiency is between 39.4-42.9%, and the efficiency for re-heat steam energy storage plan is between 51.3-51.4%.

Table 4. Storage efficiencies of main steam energy storage under different reloading and unloading speeds

Generation steam in the unloading process [th ⁻¹]	Extraction steam in reloading process[th ⁻¹]			
	50	100	150.0	176.4
100	41.0%	41.4%	42.2%	42.9%
200	40.6%	40.9%	41.7%	42.4%
300	40.4%	40.7%	41.5%	42.2%
415	39.4%	39.7%	40.5%	41.2%

Table 5. Storage efficiencies of re-heat steam energy storage under different reloading and unloading speeds

Generation steam in the unloading process [th ⁻¹]	Extraction steam in reloading process [th ⁻¹]	
	50	76.4
20	51.4%	51.4%
40	51.3%	51.3%
60	51.3%	51.3%

Exergy analysis

Considering the MSES system efficiencies depend on the reloading and unloading speeds but varying within a small range, in this study, the storage efficiency of a specific MSES system is defined as the efficiency when the reloading speed is the maximum. The exergy analysis is conducted based on simulation results.

The exergy loss analyses of MSES systems are shown in figs. 9 and 10. The simulation results show that the main energy loss comes from the throttling process after the steam mixes into the turbine system, reaches up to 16.417 MW and 9.195 MW, respectively. Figure 11 shows that the throttling process in the T-S diagram.

Then in the main steam energy storage plan, the exergy loss in the unloading heat exchanger is also considerable, which is 1.374 MW. According to the Q-T diagram in the heat transfer process in fig. 12, apparently the heat transfer temperature difference in the unloading cycle is too high, it causes large exergy loss, which results in the low efficiency of the whole storage cycle.

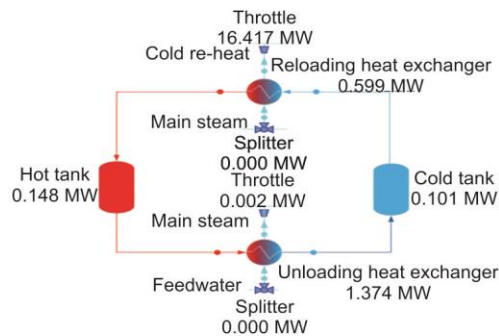


Figure 9. Exergy loss in the MSES system for main steam energy storage

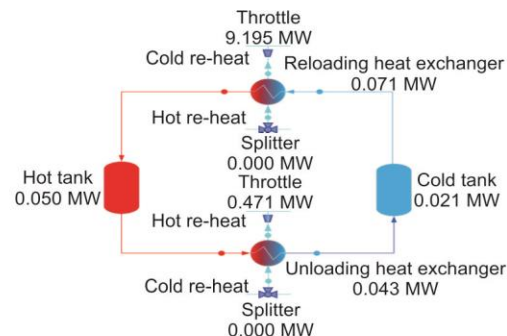


Figure 10. Exergy loss in the MSES system for re-heat steam energy storage

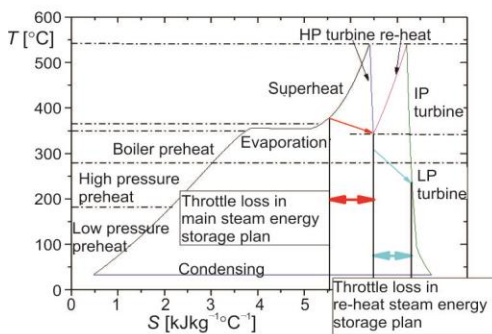


Figure 11. The T-S diagram of the Rankine cycle

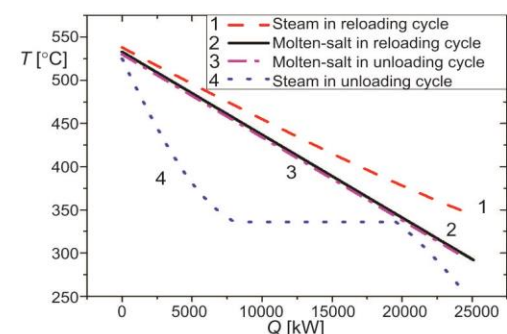


Figure 12. The Q-T diagram of the heat transfer process in the main steam storage plan

Optimized steam energy storage

Based on the simulation results and exergy analyses of steam energy storage plans, the main reason for the throttle loss is that the exhaust steam out of the heat exchanger has to go to a lower pressure point in the system, which causes the exergy loss of the MSES system. In this section, the optimized plans for both main steam and re-heat steam were proposed to improve storage efficiencies.

Main steam energy storage

Based on the analysis of the main steam storage plan, a similar scheme with multi-stage heat exchangers is proposed. The steam condenses into water and is led into the feed-water pipe. As shown in figs. 13 and 14, instead of using just one heat exchanger, the new plan separates the reloading and unloading heat transfer process into three steps with middle buffer tank, so the molten-salt mass-flow could be adjusted in different heat transfer process. As shown in fig. 14, the steam evaporating temperature in the unloading process (75% THA) should be lower than the condensation temperature in the reloading process (30% THA), thus instead of the normal sliding pressure operation given in tab. 1, in the reloading process, the main steam pressure should be fixed and kept the same as the design working condition, which is 16.67 MPa.

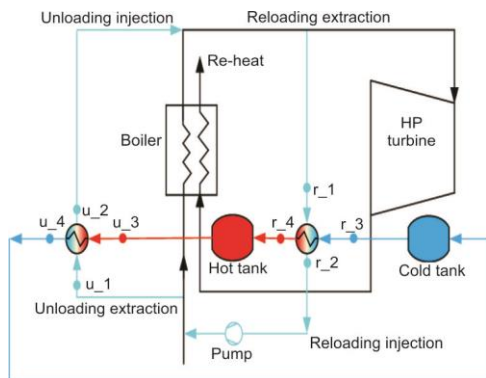


Figure 13. Optimized main steam energy storage plan

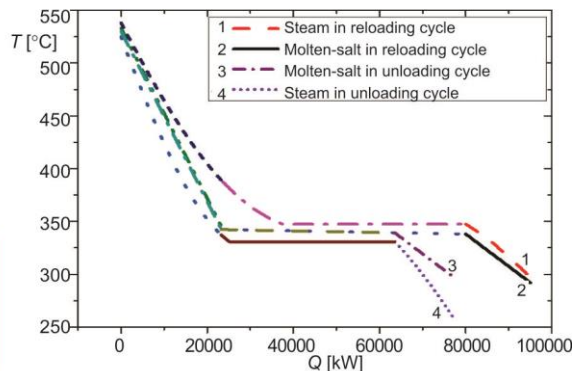


Figure 14. The Q-T diagram of the heat transfer process in the optimized main steam storage plan

According to the optimized plan of main steam energy storage, in the reloading process, with the increase of the extraction steam mass-flow into the MSES system, the main steam is nearly unchanged, but the re-heat steam would decrease gradually, which causes the re-heat temperature rise. As shown in figs. 15 and 16, the maximum re-heat temperature is 546 °C, which determined the maximum extraction steam mass-flow for the MSES system is 137.2 t/h, and the electrical power decreases from 177.2 MW to 142.1 MW, the reduction of the MOL is 35.1 MW, about 5.9% of the rated load.

As for the unloading operation limit, it is the same as the simple main steam energy storage plan in fig. 17. The simulation result in tab. 6 shows that the storage efficiency has increased up to 72.6%.

Re-heat steam energy storage

Considering the exhaust steam in the reloading cycle is at the energy level of cold re-heat, but the pressure is a little lower, therefore it has to go into the deaerator and

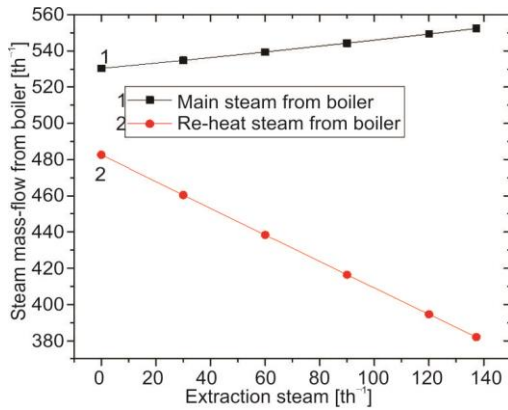


Figure 15. Steam generation from boiler for optimized main steam energy storage

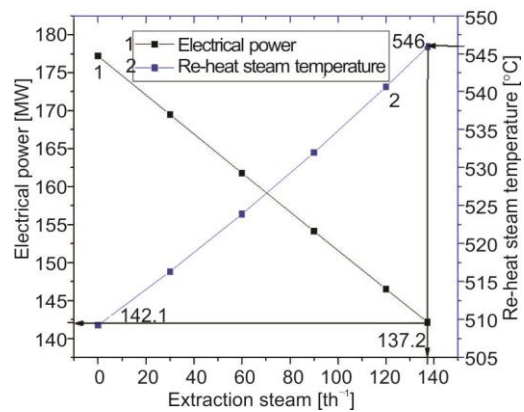


Figure 16. Operational limit in the reloading process for the optimized main steam energy storage system

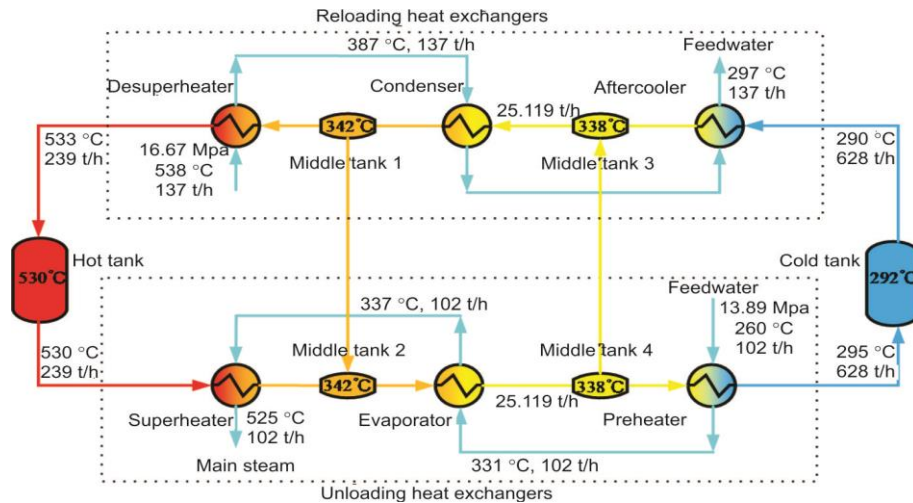


Figure 17. Reloading operational limit for optimized main steam energy storage plan

low-pressure preheaters, which causes exergy loss, also the lower storage efficiency. In order to improve storage efficiency, a new scheme with an extra compressor is proposed in fig. 18. Keeping the thermodynamic parameters the same as the plan in fig. 2, the exhaust steam is introduced into the compressor and mixed with cold re-heat steam eventually.

The re-heat steam in the boiler increases with the extraction steam into the MSES system increasing, which would lead that the re-heat temperature decreases. In order to keep the hot molten-salt temperature high enough to heat the cold re-heat steam in the unloading process, the re-heat temperature should not be lower than 500 °C. As shown in figs. 19 and 20, the maximum extraction steam mass-flow is 53.0 t/h, and the electrical power decreases from 177.2 MW to 174.2 MW, the reduction of the MOL is 3.0 MW, about 0.5% of the rated load.

The simulation results in tab. 7 show that by avoiding energy level downgrade in the storage system, the storage efficiency increases up to 78%.

Table 6 Simulation results of optimized main steam storage plan with maximum reloading speed

Thermal parameters	Values
Output power decrease in the reloading cycle [MW]	35.1
Output power increase in the unloading cycle [MW]	25.5
Storage efficiency [%]	72.6
Molten-salt mass-flow for reloading process [th ⁻¹]	239/25119/628
Molten-salt mass-flow for unloading process [th ⁻¹]	239/25119/628
Extraction steam mass-flow for reloading process [th ⁻¹]	137.2
Generated steam mass-flow for unloading process [th ⁻¹]	102.2

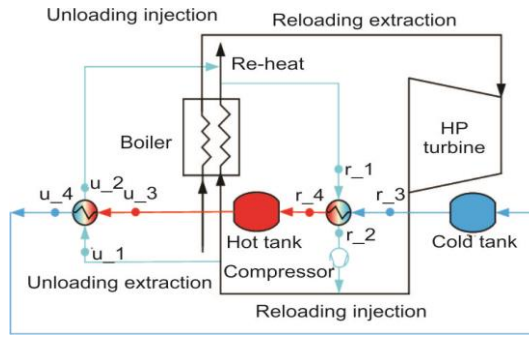


Figure 18. Re-heat steam energy storage plan with compressor

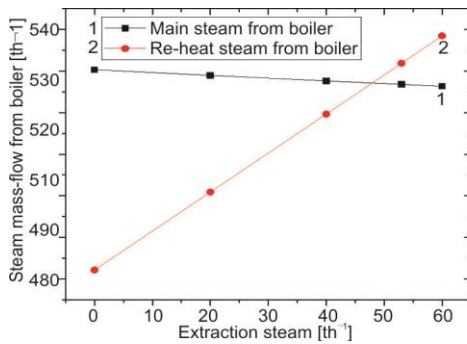


Figure 19. Steam generation from boiler for optimized re-heat steam energy storage

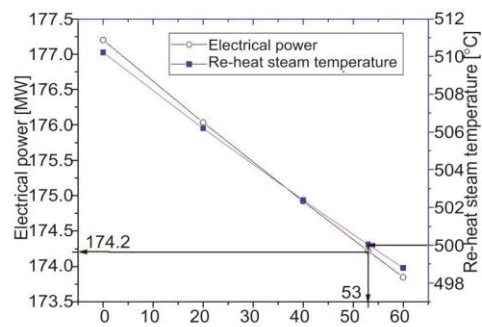


Figure 20. Operational limit in the reloading process for the optimized re-heat steam energy storage system

Table 7. Simulation results of optimized re-heat steam storage plan with maximum reloading speed

Thermal parameters	Values
Output power decrease in the reloading cycle [MW]	3.0
Output power increase in the unloading cycle [MW]	2.4
Storage efficiency [%]	78
Molten-salt mass-flow in the reloading process [th ⁻¹]	69.7
Molten-salt mass-flow in the unloading process [th ⁻¹]	69.7
Extraction steam mass-flow for reloading process [th ⁻¹]	53.0
Generated steam mass-flow for unloading process [th ⁻¹]	48.5

Coupled MSES plan

The simulation results show that the optimized main steam and re-heat steam energy storage plan would cause the re-heat temperature to increase and decrease in both reloading and unloading processes, respectively. With the coupled plan shown in fig. 21 and the appropriate ratio between the two main steam and re-heat steam MSES system capacities, it is possible to avoid boiler re-heat overhear issue and turbine axial unbalance problem. Figure 22 gives the mass-flow relation between the main steam and re-heat steam ratio at normal working conditions, and it should also be obeyed when adjusting the mass-flow extraction into the MSES system.

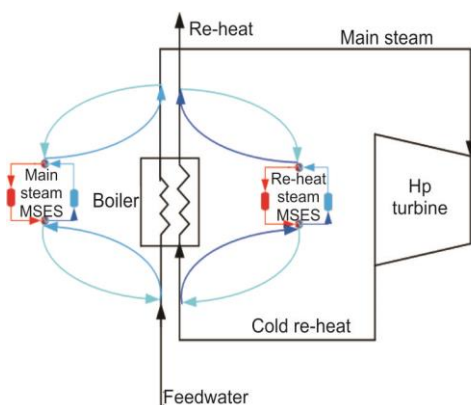


Figure 21. Coupled MSES plan

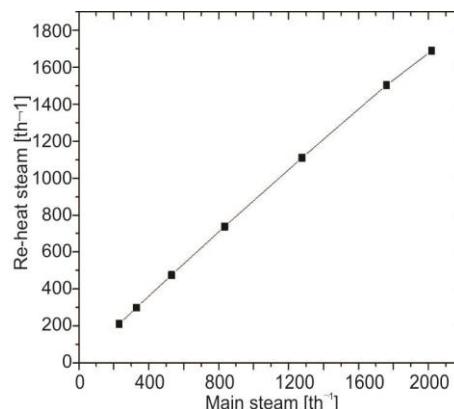


Figure 22. Mass-flow relation between main and re-heat steam at normal working conditions

For the coupled plan, the steam out of boiler could be reduced without affect to the CFPP, so the reloading limit depends on the minimum steam mass-flow requirement of the turbine, based on the design data, the turbine requires that the lowest exhaust mass-flow is 240th⁻¹ to keep the last stage blade (LSB) of the turbine from overheating.

Based on the mass-flow requirement for LSB, the simulation results of the coupled MSES system are listed in tab. 8. The MOL could be reduced by 80.7 MW, which is about 13.5% of the rated load, with 75.1% storage efficiency.

Table 8. Simulation results of coupled MSES system

Thermal parameters		Values	
Output power decrease in the reloading cycle [MW]		80.7	
Output power increase in the unloading cycle [MW]		60.6	
Storage efficiency [%]		75.1	
		Main steam MSES	Re-heat steam MSES
Reloading process	Extraction steam mass-flow [th ⁻¹]	171.6	151.3
	Molten-salt mass-flow [th ⁻¹]	299/31408/785	198.9
Unloading process	Generated steam mass-flow [th ⁻¹]	127.8	118.5
	Molten-salt mass-flow [th ⁻¹]	299/31408/785	198.9

Conclusions

In this paper, novel MSES systems integrated with a subcritical 600 MW CFPP were proposed, thermodynamic simulation and exergy analysis were performed to explore the en-

ergy storage efficiency and MOL reduction potential for the CFPP. The results would give a complete depiction of the system characteristics of the MSES. To be specific, the following conclusions could be drawn.

- Thermodynamic analysis of the simple MSES system is performed, and it is found that with main steam, re-heat steam energy storage systems, the MOL decreases by 27.2 MW, 10.6 MW, the energy storage efficiencies are 39.4-42.9% and 51.3-51.4%, respectively. The exergy analysis of the MSES system reveals a larger exergy loss in the throttling process when exhaust steam out of the reloading heat exchanger mixing with the low pressure steam in the Rankine cycle. For the main steam plan, the heat transfer exergy loss is also considerable. The exergy analysis provides a guide for the optimization of advanced MSES systems.
- Optimized integrations of MSES systems and CFPP with higher efficiencies are then proposed. The exhaust drains, or steam is compressed and lead into high pressure points in the system. For the main steam plan, the heat transfer energy loss is reduced with multistage heat exchangers and buffer storage tanks. With the optimized plans, for main steam and re-heat steam plans, the storage efficiencies are 72.6% and 78%, the MOL decreases by 35.1 MW and 3 MW, respectively.
- The maximum MOL reduction potential of the MSES system was analyzed in this paper. With a coupled including both main steam and re-heat steam energy storage, the MOL reduction depends on the mass-flow requirement for the LSB, the results show that with the coupled plan, MOL decreases by 80.7 MW, and storage efficiency is 75.1%.
- Based the calculation in this paper, integrating MSES system with the steam cycle in the CFPP is feasible to reduce the MOL, and by optimizing the MSES system scheme, it is possible to achieve higher efficiency with higher investment cost, there should be a detailed technical economy analysis for each potential project. Dynamic simulation and experiment is the next phase to explore the possibility of using MSES as a primary frequency control power source.

Acknowledgment

The authors would like to thank Xi'an Thermal Power Research Institute for providing details on the cycle of the power plants used in this paper. This paper is supported by the National Key R&D Program of China NO. 2017YFB0902100.

Nomenclature

A	– area [m^2]
e	– specific enthalpy [kJkg^{-1}]
h	– specific enthalpy [kJkg^{-1}]
k	– heat transfer coefficient, [$\text{Jm}^{-2}\text{C}^{-1}$]
$LMTD$	– mean logarithmic temperature difference [$^{\circ}\text{C}$]
m	– mass-flow rate, [th^{-1}]
p	– pressure [MPa]
QR	– radiation flow [W]
s	– specific entropy [$\text{kJkg}^{-1}\text{K}^{-1}$]
T	– temperature [$^{\circ}\text{C}$]
v	– volume flow [m^3s^{-1}]
W	– power [W]

Greek symbol

η	– energy storage efficiency [%]
--------	---------------------------------

Subscripts

r	– reloading
u	– unloading
0	– reference state

Acronyms

CFPP	– coal-fired power plant
CAES	– compressed air energy storage
MSES	– molten-salt energy storage
TES	– thermal energy storage
THA	– turbine heat acceptance
MOL	– minimum operation load

References

- [1] Gonzalez-Salazar, M. A. *et al.*, Review of the Operational Flexibility and Emissions of Gas- and Coal-Fired Power Plants in a Future with Growing Renewables, *Renewable and Sustainable Energy Reviews*, 82 (2018), Part 1, pp. 1497-1513
- [2] Diaz-Gonzalez, A. *et al.*, A Review of Energy Storage Technologies for Wind Power Applications, *Renewable & Sustainable Energy Reviews*, 16 (2012), 4, pp. 2154-2171
- [3] Chen, H., *et al.*, Progress in Electrical Energy Storage System: A Critical Review, *Progress in Natural Science: Materials International*, 19 (2009), 3, pp. 291-312
- [4] Beaudin, M., *et al.*, Energy Storage for Mitigating the Variability of Renewable Electricity Sources: An Updated Review, *Energy for Sustainable Development*, 14 (2010), 4, pp. 302-314
- [5] Tian, Y., Zhao, C. Y., A Review of Solar Collectors and Thermal Energy Storage in Solar Thermal Applications, *Applied Energy*, 104 (2013), Apr., pp. 538-553
- [6] Gil, A., *et al.*, State of the Art on High Temperature Thermal Energy Storage for Power Generation. Part 1—Concepts, Materials and Modelling, *Renewable and Sustainable Energy Reviews*, 14 (2010), 1, pp. 31-55
- [7] Medrano, M., *et al.*, State of the Art on High-Temperature Thermal Energy Storage for Power Generation. Part 2—Case Studies, *Renewable and Sustainable Energy Reviews*, 14 (2010), 1, pp. 56-72
- [8] Garbrecht, O., *et al.*, Increasing Fossil Power Plant Flexibility by Integrating Molten-Salt Thermal Storage, *Energy*, 118 (2017), Jan., pp. 876-883
- [9] Al-Maliki, W. A. K., *et al.*, Modelling and Dynamic Simulation of a Parabolic Trough Power Plant, *Journal Of Process Control*, 39 (2016), Mar., pp. 123-138